Iraqi Journal of Biotechnology, 2017, Vol. 16, No. 3, 31-45

DsDNA-encased single walled carbon nanotubes (SWNTs) biosensor for detecting hydrogen peroxide in biological environment

Azhar Kamel

The Ministry of Science and Technology

Received: 13 August 2017 / **Accepted**: 10 October 2017

Abstract: Hydrogen peroxide is a ubiquitous molecule. We exhale it, and take it in from our diet, and excrete it. It plays an important role in physiological and pathological processes. H_2O_2 is closely related to several human diseases including cancers. Single-walled carbon nanotubes (SWNTs) have drawn great interest in chemical and biological optical sensor applications due to their novel near infrared (NIR) optical properties that are extremely sensitive to the surrounding environment. Herein, DsDNA-encased SWNTs for detecting hydrogen peroxide in a biological environment: dsDNA-SWNTs have been used as a bio-probe sensor for optical detection of H_2O_2 in a blood model matrix (BMM) and serum, It has been found that, 1.7 M thiocyanate ion (SCN^-) and 1 mM nitrite ion (NO_2^-) have shown the ability to initiate and accelerate the reaction as well as the restoration of suppressed spectral intensity of SWNT. It has been found that, the detection limits (dl) of H_2O_2 in BMM-1.7 SCN^-, BMM-1 mM nitrite ion, and serum were 5.8, 9.4, and 2.9 μM, respectively and thus have the sensitivity required to detect physiological and environmental of H_2O_2.

Keywords: Single-walled carbon nanotubes, hydrogen peroxide, serum, thiocyanate ion, nitrite ion, optical sensors, near infrared

Corresponding author: should be addressed (Email: azhaar_abed@yahoo.com)

Introduction:

Carbon nanotubes exhibit unique electronic, optical, and electrical properties. These properties make them ideal candidates for sensors to detect various biological molecules. Single-walled carbon nanotubes -SWNTs exhibit many intrinsic optical properties such as optical absorption and fluorescence in the novel near infrared - NIR range of 820-1600 nm. At NIR, their absorption by biological tissues is often minimal, and the inherent photostabilities of SWNTs is a desirable attribute for the design of *in vitro* and *in vivo* sensors.(1, 2) However, due to their poor solubility in most solvents, The use of SWNTs for promising applications as biosensors is difficult.(3) Stable, homogeneous, aqueous dispersions of individual SWNTs can, nevertheless, be obtained by ultrasonication of mixtures of surfactants or DNA and carbon nanotubes in water.(4) Recently, systems consisting of SWNTs and DNA have been rapidly expanded and are still the focus of important research efforts.(5) Both DNA strands and CNTs are prototypical one-dimensional structures. DNA plays a central role in biology, and CNTs hold promise for an essential role in nanotechnological applications. DNA and CNTs have complementary structural features that

make it possible to assemble them into a stable hybrid structure. This fact has motivated many studies and possible applications.(6) It has been found that DNA-encased SWNTs are optically sensitive to hydrogen peroxide.(7, 8) Hydrogen peroxide is important because it is considered as an essential mediator in many fields such as the food, pharmaceutical, clinical, industrial, and environmental analysis fields.(9) It can be found in drinking water, rain , and sea water.(10) It is a friendly oxidizing agent to treat a large number of pollutants. It is used as an antimicrobial agent and as a sterilizing agent on the foil lining of aseptic packages containing food products. The final product of aseptic packages must not contain greater than 14.7 mM H_2O_2.(11) In living systems, H_2O_2 plays an important role in physiological and pathological processes.(12) Compared to other reactive oxygen species (ROS), H_2O_2 is a dominant oxidant in cellular redox signaling processes due to the fact that it has a much longer lifetime (1 ms half-life) and higher concentration (100 nM at steady-state level) than other ROS such as superoxide and the hydroxyl radical.(13) It can also be cytotoxic (with a level of >50 μM) to a wide range of animal, plant, and bacterial cells in culture. The levels of hydrogen peroxide in fresh human urine range from 0.4-109.6 μM.[10] High contractions of H_2O_2 cause several human diseases, including Alzheimer's disease,(14) cardiovascular disorders,(15) and cancers.(16) Therefor, methods that can measure H_2O_2 rapidly, simply, and precisely represent valuable tools for H_2O_2 assessment. Numerous electrochemical biosensors for H_2O_2 have been developed based on modified electrodes as summarized in a recent review article.(17) Similarly, SWNTs and their modified electrodes have been widely used as electrochemical sensors to detect H_2O_2 (18-20). Also, several analytical methods, including fluorescence spectroscopy (21,22), spectrophotometry (23) and chemiluminesence (24) have been developed to detect H_2O_2. However, these methods have several disadvantages. Included in these disadvantages is electrode kinetics too slow and overpotentials too high for what is required of redox reaction of H_2O_2 on many electrodes materials, interferences, long pre-treatments of the sample, and the utilization of toxic or expensive reagents.(25) Herein, sensitive, rapid, and low cost methods have been used to detect H_2O_2 in BMM and serum. The detection was done by monitoring the NIR absorption spectral intensity of dsDNA-SWNTs at 1280 nm, which comes from the first interband transition of semiconducting SWNTs. The proposed mechanism and the detection limits are presented in this work.

Experimental Section

Materials

Raw HiPco SWNTs (lot no. R0496, 2005) were purchased from Carbon Nanotechnologies, Inc. Their diameters ranged from 0.7 to 1.1 nm, and they were a few hundred nanometers long. Double-stranded deoxyribonucleic acid (dsDNA from salmon testes) was obtained from Sigma. Sodium phosphate, hydrochloric acid, and sodium hydroxide were acquired from Fisher Scientific®. Acid and base solutions of 0.1 M and 1.0 M were used

to adjust the pH at 7.0; an Orion model 420A pH meter with an Orion Thermo Scientific microprobe electrode was used to detect pH levels. BMM was prepared using the following components: bovine serum albumin (BSA) (purchased from Sigma-Aldrich®), glucose and 99 % triacetin (purchased from ACROS), activation agents like 99.99% sodium thiocyanate (NaSCN) (purchased from ACROS), 97 % sodium nitrrite ($NaNO_2$) (purchased from Fisher Scientific®), Hydrogen peroxide 30 wt % hydrogen peroxide (H_2O_2, ACS) 30 (purchased from ACROS). The UV-VIS-NIR absorption spectra were measured in all samples on a Varian Cary 5000 UV-VIS-NIR spectrophotometer.

Preparation of dsDNA Encased HiPco SWNT Suspensions

In a typical experiment, 1.0 mg of pristine HiPco SWNTs and 3.5 mg dsDNA were mixed with 5 ml of a 50 mM phosphate buffer. The pH of the phosphate buffer was adjusted to 7.0 by adding 0.1 M NaOH and 0.1 M HCl. The sample was ultrasonicated in an ice-water bath for 1.5 hours (Sonics model VCX 130 PB, 20 kHz, output power ~8 W) to disperse the nanotubes. The sample was subjected to centrifugation at 14,000 rpm (VWR Galaxy16 Microcentrifuge) for 16 hours. The optical density (OD) of SWNT stock solutions was ~0.3. The OD of suspension after the addition of all of the required reagents was fixed to be ~0.03. The UV-VIS-NIR absorption spectrum was measured on a Varian Cary 5000 UV-VIS-NIR spectrophotometer with the phosphate buffer as the background. Three distinguished absorption bands in the NIR were obtained at roughly 1130 nm, 1190 nm and 1275 nm (Figur 1 a). These belong mainly to the first interband transitions (S_{11}) of (9, 4), (12, 1), and (10,5) semiconducting nanotubes, respectively.(26-28) The band of ~1275 nm was chosen to study the optical properties of dsDNA-SWNT-H_2O_2 in BMM and serum. The band of 732 nm was chosen to normalize all absorption spectra, for the correction of dilution effects.

Solutions for BMM –Related Experiments

The components of BMM were selected to mimic human plasma composition with 2.320 g/l triacetin, 66.5 g/l BSA, and 10 mM glucose. Triacetin and BSA were used to represent the triglyceride and blood protein, respectively.(29) A fresh stock solution of BMM was prepared in 50 mM phosphate buffer at pH 7.0 by dissolving the appropriate weight of triacetin, BSA, and glucose to achieve concentrations of 2.963 g/L, 85g/L, and 12.79 mM, respectively. Also, the solutions from each component of BMM were also prepared individually. To study the reaction of H_2O_2 and SWNTs in BMM, 0.035 ml of dsDNA-SWNT suspensions, 0.275 ml of fresh stock BMM (or one of its components), and 0.010 ml of H_2O_2 solutions were mixed immediately into 1 mm quartz cells for optical measurements. The phosphate buffer was used to keep the total volume of 0.35 ml. Surprising data were observed when the S_{11} bands of dsDNA-SWNTs in BMM became insensitive to both high and low concentrations of H_2O_2 (Figure 1 b).

Solutions for Activation Agents-Related Experiments

Many chemical agents were studied in the context of triggering SWNTs-H_2O_2 reactions in BMM. For studying the sensitivity of the SWNTs-H_2O_2 reaction to SCN^- and, a series of stock solutions of selected agents and H_2O_2 were prepared.

Serum-Related Experiments

In a typical experiment, 0.275 ml of serum, 0.35 ml of dsDNA-SWNT, and 0.010 ml of a specific concentration of H_2O_2 were used; the phosphate buffer was used to keep the total volume at 0.35 ml. For the sensitivity study, a series of H_2O_2 solutions were prepared with a wide range of concentrations (0.5-8750) ppm. The sample was immediately mixed in a 1 mm path length quartz cell, and the time-dependent absorption spectrum was measured on the UV-VIS-NIR spectrophotometer.

Results And Discussion

Optical Characterization of dsDNA-SWNT with H_2O_2 in BMM

In this work, it was observed that the S_{11} bands of dsDNA-SWNTs became insensitive to H_2O_2 in BMM solution (Figure 1b). In order to identify the main component which may deactivate the reaction of SWNTs with H_2O_2, the effect of each component of BMM was tested separately. These data are shown in Figure 2, where the decay curve of the 1274-1280 nm band of SWNTs in solution with different components of BMM is shown. Our results show that the reaction of SWNTs and H_2O_2 occurred in the phosphate buffer, glucose, and triacetin, but not in BSA. This suggests that BSA is the component deactivating the reaction in BMM. The observed reaction between SWNTs and H_2O_2 suggests that there is a strong electron withdrawal from the nanotube valence band by H_2O_2, and also that none of the components of BMM except BSA impede the reaction. In SWNT suspensions containing BSA, the reaction of protein with H_2O_2 might take place as a result of BSA antioxidant action. Albumin may have an antioxidant in plasma related to its high concentration.(30) To study the effect of the antioxidant behavior, a suspension of SWNTs was prepared by adding 100 ppm H_2O_2 to dsDNA-SWNTs (left for 24 hours), and then 0.275 ml of BMM and BSA were added to the suspension. The spectral intensity was suppressed due to the reduction in SWNT S_{11} transitional strength by H_2O_2. This study is presented in Figure3, where there are two observations that can be made: 1) The restoration of the suppressed spectral intensity of SWNT S_{11} occurred within the reaction time after the addition of BSA or BMM. 2) A 6 nm red shift of SWNT S_{11} from 1275 to 1280 nm was observed. As H_2O_2 is deactivated by antioxidant, the SWNT original band gap and transitional strength are restored, and the suppressed S_{11} spectral intensity is recovered. While in BSA, the red shift suggests that the BSA may coat the nanotubes by replacing the dsDNA strand, and might prevent H_2O_2 from forming charge transfer complexes with dsDNA-SWNTs leading to the restoration of S_{11} spectral intensity. Other work has shown that BSA can be immobilized on SWNTs.(31) Also,

BSA can work as an antioxidant, the main feature responsible for the antioxidant role of BSA is the thiol group(30). Albumin contains one thiol group per molecule, and this is the major source of protein thiol in plasma. The thiol group of BSA has been shown to be accessible to electrophilic agents such as peroxides.(30) We observed that the dsDNA-SWNT-BSA samples started to react with H_2O_2 at 0.08504 g/l BSA. Figure 4 shows a small decrease in the S_{11} spectral intensity with the reaction time at this concentration of BSA. It has been shown that the reaction of the thiol with hydrogen peroxide in human serum albumin follows the pseudo first-order reaction.(32) For that, sensing H_2O_2 in biometrics by using the optical properties of SWNT must be enhanced. Some chemical agents were tested in order to achieve that purpose.

Activation of the Reaction of dsDNA-SWNTs and H_2O_2 in BMM

Figure 5 shows the preliminary result of the dsDNA-SWNTs-1.0 w% H_2O_2 in BMM after adding 1.0 M SCN^-. It was shown that before adding SCN^-, SWNTs in BMM are not sensitive to H_2O_2. When SCN^- ions are added, the reaction starts and is accelerated, finishing in near one minute. Similar behavior was observed with nitrite ion. Figure 6 shows the preliminary result of the dsDNA-SWNTs-200 ppm H_2O_2 in BMM after adding 0.1 M NO_2^-.

Thiocyanate Ions (SCN^-)

In Figure 7**,** 200 ppm of H_2O_2 and 1.7 M of SCN^- were added to the SWNT in BMM, it was observed that the spectral intensity of the three S_{11} bands decreases rapidly during the initial reaction period with H_2O_2 (Figure 7a), but then the suppressed spectral intensity starts to recover after about 35 min and fully recovers after 160 min (Figure 7b). SCN^- is an antioxidant and not react with SWNT. [33]Figure S4 shows the spectral intensity of SWNT with 1.7 M of SCN^-. In Figure 8, the effect of SCN^- concentration was studied. The results demonstrated that the SCN^- accelerates both the spectral suppression and recovery rate until a maximal SCN^- concentration is reached at about 1.7 M. A concentration higher than 1.7 M causes precipitation in the samples due to the ability of SCN^- to precipitate BSA.[34]The restoration of the suppress NIR spectra is faster at higher SCN^- concentrations. At 1.7 M of SCN^-, the SWNTs' response to H_2O_2 was completely reversible. The response time of dsDNA-SWNTs in the BMM was on the order of a few minutes, while the recovery time ranged from several minutes to a few hours depended on the concentration of SCN^-. The system of SWNT-BMM-1.7 M SCN can detect H_2O_2 as low as 10 ppm (Figure 9). The result shows that the spectral intensity of the 1280 nm restored after adding H_2O_2 at each concentration. The time needed to fully restore was increased with H_2O_2 concentration. The standard curves of the 1280 nm were established by plotting ($\Delta A/A_0$) ($\Delta A = A_0 - A_{15\ min}$) as a function of [$H_2O_2$], which shows a linear relationship (Figure 10).

Nitrite Ion (NO_2^-)

Figure 11 shows the typical spectrum of 1 mM nitrite ion in the system of SWNT-BMM-200ppm H_2O_2.

1 mM nitrite ion decreased the spectral intensity at NIR slower than SCN^- and the restoration process was occurring very slowly. This could be related to the low concentration of nitrite ion compared to the concentration of H_2O_2 (35, 36). The system of SWNT-BMM-1mM nitrite can detect H_2O_2 as low as 0.5 ppm (Figure 12). The result shows that the spectral intensity at the 1280 nm restored after adding H_2O_2 at each concentration. It is interesting to note that the sensitivity (estimated as A_t/A_0 at 1280 nm) for H_2O_2 observed in the SWNT-BMM-1mM nitrite was higher than that observed for SWNT-BMM-1.7 M of SCN^-. The standard curves of the 1280 nm were established by plotting ($\Delta A/A_0$) ($\Delta A = A_0 - A_{60}$) as a function of log[H_2O_2], which shows a linear relationship (Figure 13). The reaction of H_2O_2 with nitrite ion lead to produce the peroxynitrite ($ONOO^-$) which considers as a strong oxidant.(37, 38) The working mechanism of nitrite ion might relate to the reaction of $ONOO^-$ with SWNTs. On the other hand, peroxynitrite can damage the protein[f] and attack on sulfhydroyl groups and thioethers, and causing hydroxylation and nitrosation of aromatic amino acids containing essential residues in proteins.(39). Overall, the reactions of H_2O_2 will lead to the consumption of H_2O_2 and restores the spectral intensity of SWNTs.(37)

Serum Related Experiments

BMM was selected to mimic serum composition. In this part, we studied the detection of H_2O_2 in a system of SWNT-Serum. Figure 14 shows the time dependent spectrum of 100 ppm H_2O_2 with SWNT-Serum. The spectral intensity of the three S_{11} shows similar behavior of the reaction of SWNT-BMM-H_2O_2 in the presence of SCN^-. The spectral intensity S_{11} suppressed rapidly during 15 min after adding 100 ppm H_2O_2 (Figure 14a), then the suppressed spectral intensity starts to recover after 15 min and the fully recovers was not occurred up 24 hours (Figure 14b). The system of SWNT-serum can detect H_2O_2 as low as 0.5 ppm (Figure 15). A range of H_2O_2 from 0.5-50 ppm showed a dramatic suppression of the SWNT spectral intensity at 1280 nm during the initial reaction period with H_2O_2 , then the suppressed spectral intensity starts to recover after about 30 min and fully recovers was occurred at low concentration of H_2O_2 (Fig. 15 a). However, the unique data were observed when the concentration of H_2O_2 was >50 ppm, the suppression of SWNT spectral intensity starts to decrease with the increasing of H_2O_2 concentration (Fig. 18 15 b). The response of SWNTs stopped at 5000 ppm H_2O_2. It can be noticed that the highest response occurred at 50 ppm then started to decline at 100 ppm..The standard curves of the 1280 nm were established by plotting $\Delta A/A_0$ ($\Delta A = A_0 - A_{5\ min}$) as a function of [$H_2O_2$], which shows a linear relationship between (0.5-50) ppm (Figure 16).

Detection Limit Measurements

The standard curves of three systems: SWNT-BMM-Thiocyanate-H_2O_2 (system I), SWNT-BMM-Nitrite-H_2O_2 (system II), and, SWNT-Serum-H_2O_2 (system III) were established by

plotting ($\Delta A/A_0$) ($\Delta A = A_0 - A_{15\ min}$) as a function of [$H_2O_2$], ($\Delta A/A_0$) ($\Delta A = A_0 - A_{60\ min}$) as a function of Log[$H_2O_2$], and ($\Delta A/A_0$) ($\Delta A = A_0 - A_{15\ min}$) as a function of [$H_2O_2$], respectively. The standard curves of the three systems show a linear relationship. In order to calculate the detection limit, the slope *m* and the intercept *b* were obtained from the linear fit in the mentioned figures. The standard deviation *s* for system III was determined on the basis of 7 measurements of $\Delta A/A_0$ from SWNT-Serum reacting with 0.5 ppm of H_2O_2. Where *b* is the y-intercept of the standard curve, *m* is the slop and *s* is the standard deviation. Table 1 summarizes the values of *m*, *b*, *s,* and the dl equation needed for the detection limit calculations. The detection limits of the three systems based on the standard curve method and the LOD methods are summarized in Table 2. The LOD method of the system III is the most sensitive one, which has the detection limit of 0.099 ppm (2.9 µM)). The detection limit on the basis of the standard curve method can be further improved by reducing the standard deviations.

Conclusions

In this study, we have reported three different sensitive systems to detect H_2O_2 in blood model matrix (BMM) and serum depending on the unique SWNT optical properties at NIR. In BMM; triacetin, bovine serum albumin (BSA), and glucose, were selected to mimic human plasma composition. The redox reaction between SWNTs and H_2O_2 in the BMM was deactivated by BSA. SCN^- and nitrite ion were found to work as chemical agents to initiate and accelerate the reaction as well as the restoration of the suppressed SWNT spectral intensity.

In system I, SCN^- was used to accelerate both the reaction of SWNTs with H_2O_2 and the restoration of the suppressed SWNT spectral intensity in the BMM. It was determined that the optimal concentration at pH 7.0 is 1.7 M of SCN^-. The detection limit based on the LOD method was 0.2 ppm. In system II, 1 mM of nitrite ion was used to initiate the reaction of SWNT-H_2O_2 in the BMM. Without the presence of H_2O_2, nitrite ion > 1mM has shown the ability to react with SWNT and SWNT-BMM and suppressed the spectral intensity of SWNT at NIR.

The detection limit based on the LOD method was 0.32 ppm. In system III, serum was used to detect H_2O_2. The reaction of SWNT and H_2O_2 in the serum shows a unique behavior when the concentration of H_2O_2 > 50 ppm lead to decrease the suppression of SWNT absorption intensity and increase the restoration process. The detection limit based on the LOD method was 0.099 ppm.

The knowledge gaining from this work about how SWNTs react with H_2O_2 in biological solutions will provide us a useful information for developing a new, SWNT-based NIR optical H_2O_2 sensor for environmental, chemical and biological application.

Table(1): The Slope *m*, Intercept *b*, and Standard Deviation *s* for the Three System

	Detection limit (ppm)		
	System I	System II	System III
Standard Curve Method	-	-	1.39
LOD Method	0.2	0.32	0.099

Table(2): Detection limit of H_2O_2 Determined from Two Methods for the Three System.

Constants	System I	System II	System III
m	0.00438	0.218	0.00906
b	0	0.1087	0
s	-	-	0.0042
dl equation	$[H_2O_2]=3s/m$	$Log[H_2O_2]=3s-b/m$	$[H_2O_2]=3s/m$

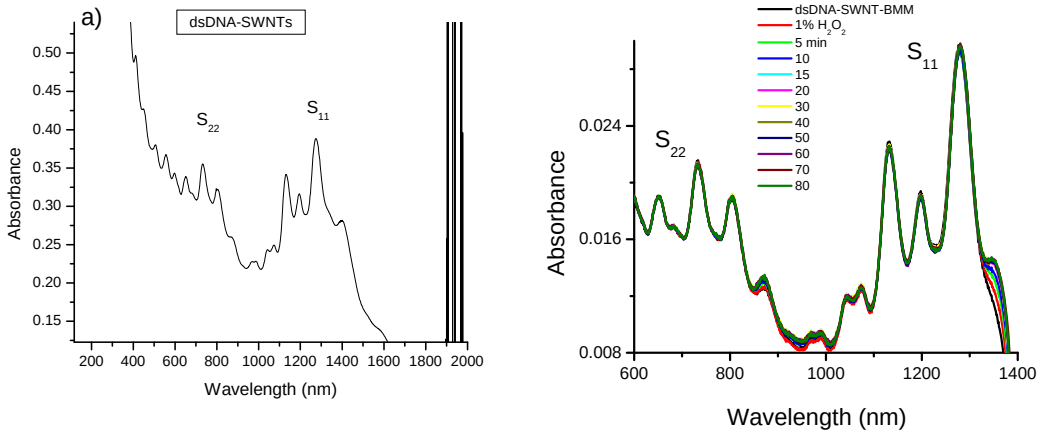

Figure (1): Absorption spectra of a) dsDNA-SWNT b) in BMM at pH 7.0 phosphate buffer as a function of time after adding 1% H_2O_2.

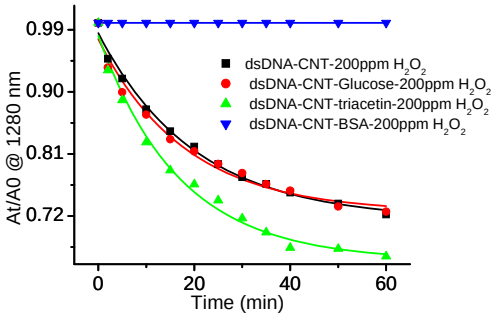

Figure (2): The decay curves at 1275-1280 nm for reaction of dsDNA-SWNT-200 ppm H_2O_2, with each BMM component. All samples were prepared at pH 7.

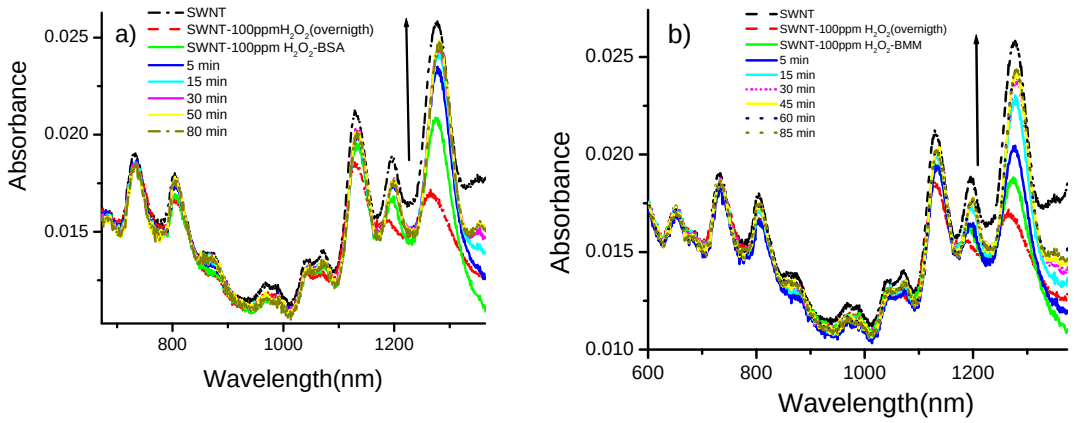

Figure (3): Restoration of optical absorption of dsDNA-SWNT-100 ppm H_2O_2 after addition of a) BSA and b) BMM prepared in phosphate buffer at pH 7.0.

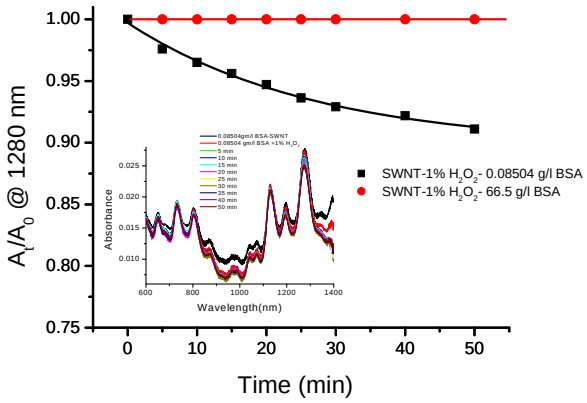

Figure (4): The decay curve at 1280 nm for a buffered dsDNA-SWNT-1% H_2O_2 in two different concentrations of BSA. The inset shows the time-dependent absorption spectra of the sample SWNT-1% H_2O_2-0.08504 g/l BSA .

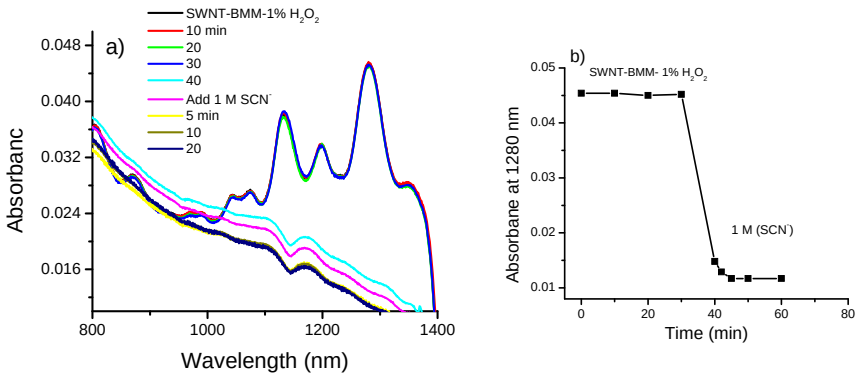

Figure (5) A: Time-dependent absorption spectra and B: Absorbance at 1280 nm changes as a function of time for a dsDNA-SWNT-BMM sample reacting with 1.0% H_2O_2 in phosphate buffer before and after addition of 1.0M SCN^-.

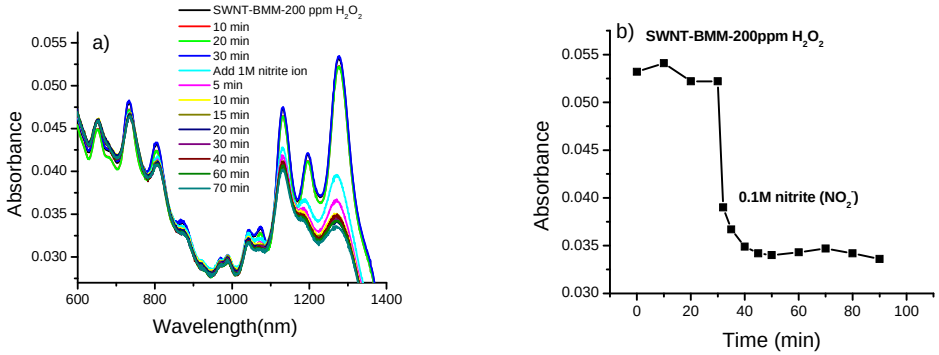

Figure (6) a) Time-dependent absorption spectra and b) Absorbance at 1280 nm change as a function of time for a dsDNA-SWNT-BMM sample reacting with 200 ppm H_2O_2 in phosphate buffer before and after adding 0.1 M NO_2^-.

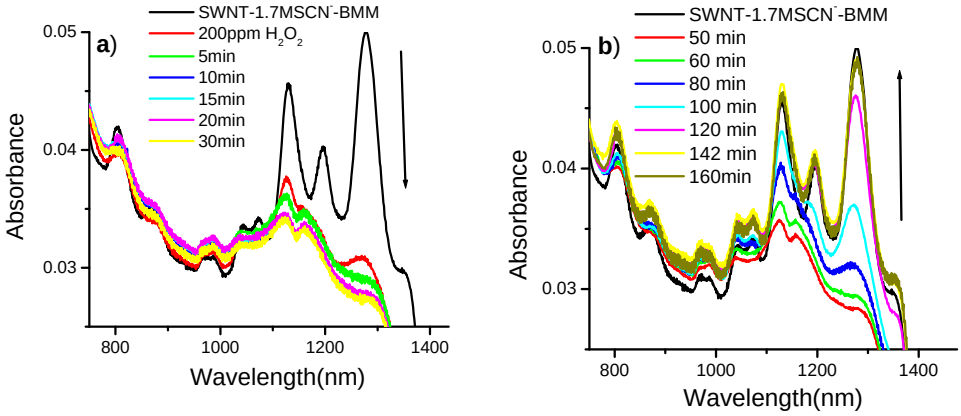

Figure (7): NIR absorption spectra of SWNT-BMM sample in phosphate buffer containing 1.7 M SCN^- changes as a function of time after addition of 200 ppm H_2O_2: (a) suppression and (b) recovery in spectral intensity.

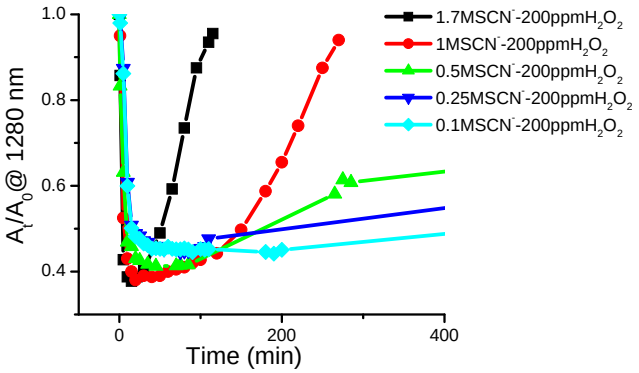

Figure (8): The spectral intensity of SWNT –BMM in phosphate buffer containing 200 ppm H_2O_2 changes as a function of time after addition of SCN^- in different concentrations. Note that the suppressed spectral intensity was restored as monitored over a period of days. Dependence on SCN^- concentrations: the higher the [SCN^-], the faster the recovery.

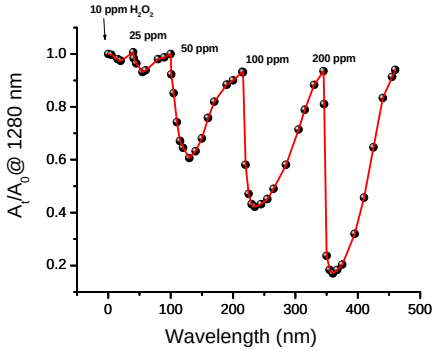

Figure (9): Spectral intensity changes of dsDNA-SWNT samples in BMM in pH 7.0 phosphate buffer containing 1.7M SCN^- after addition of different concentrations of H_2O_2.

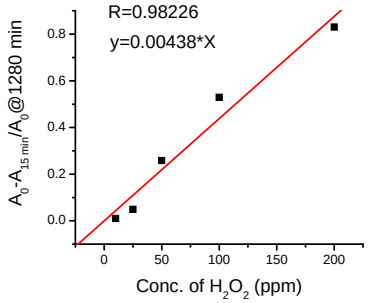

Figure (10): Standard curves of $[(A_0 - A_{15\ min})/A_0]$, plotted against $[H_2O_2]$ for SWNT-BMM-1.7 M SCN^- in pH 7.0 phosphate buffer at 1280 nm.

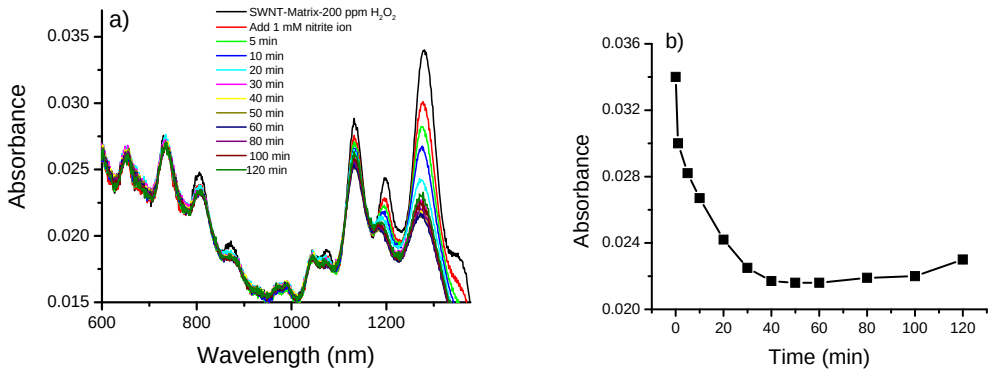

Figure (11): NIR absorption spectra of SWNT-BMM sample in phosphate buffer containing 1mM nitrite ion changes as a function of time after addition of 200 ppm H_2O_2: (a) Time-dependent absorption spectra and (b) Absorbance at 1280 nm changes as a function of time.

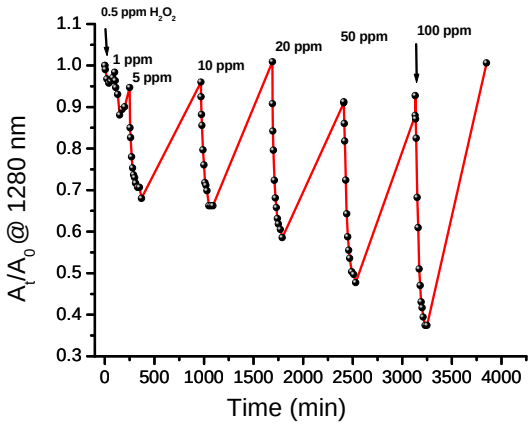

Figure (12): Spectral intensity changes of dsDNA-SWNT samples in BMM in pH 7.0 phosphate buffer containing 1 mM nitrite after addition of different concentrations of H_2O_2.

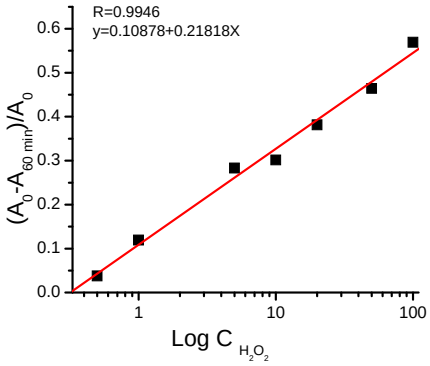

Figure (13): Standard curves of $[(A_0 - A_{60})/A_0]$, plotted against log $[H_2O_2]$ for SWNT-BMM-1 mM nitrite in pH 7.0 phosphate buffer at 1280 nm.

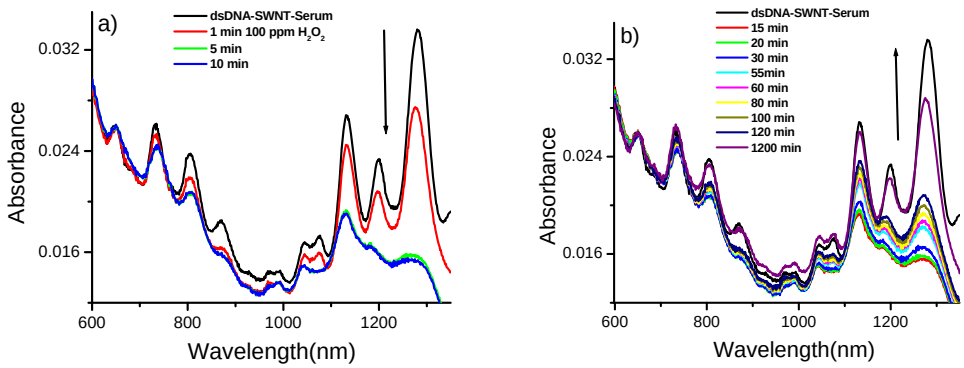

Figure (14): Time-dependent absorption spectra of SWNT-Serum-100 ppm H_2O_2 reaction a) suppressed in the SWNT spectral intensity at 1280nm; b) The restoration of the SWNT spectral intensity at 1280nm.

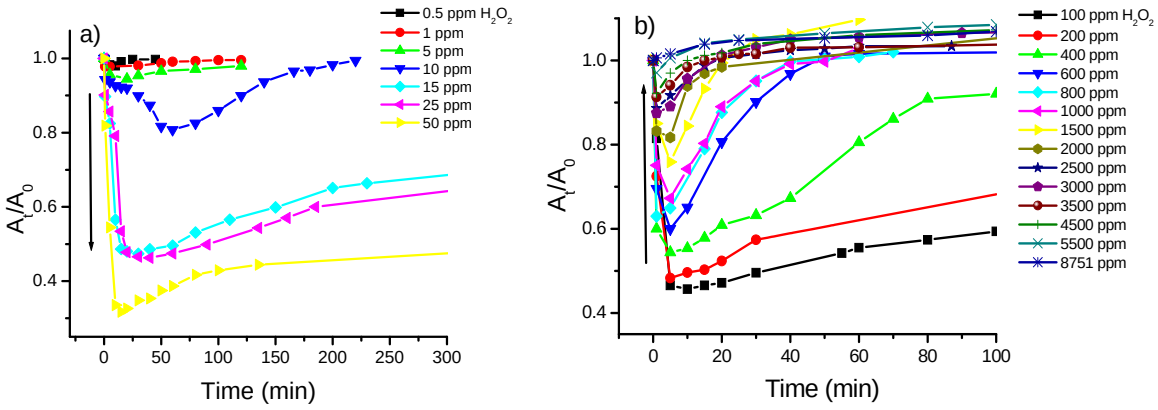

Figure (15) A: Concentration-dependent absorption spectra of SWNT-Serum reacts with various [H_2O_2] at 1280nm, B: Concentration-dependent absorption spectra become slower with increasing [H_2O_2]

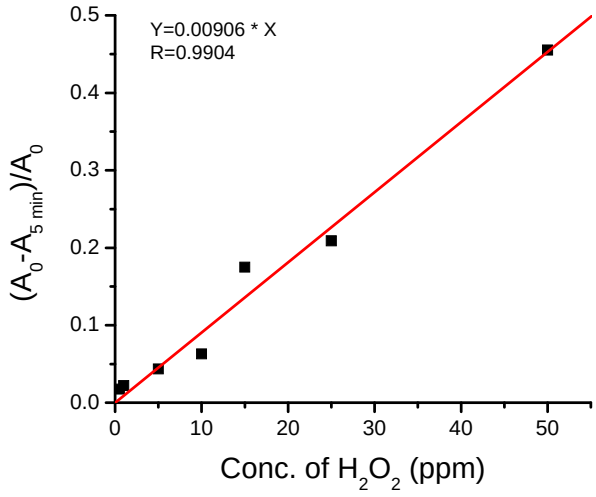

Figure (16): The Standard Calibration Curve of A_0-A_{5min}/A_0 plotted against [H_2O_2] at 1280 nm.

References

1- Wang, X. J. and Liu, Z. (2012). Carbon nanotubes in biology and medicine: An overview. ***Chinese Science Bulletin***, *57*: 167-180.

2- Boghossian, A. A.; Zhang, J.; Barone, P. W.; Reuel, N. F.; Kim, J. H.; Heller, D. A.; Ahn, J.H.; Hilmer, A. J.; Rwei, A. and Arkalgud, J.R. (2011). Near-Infrared Fluorescent Sensors based on Single-Walled Carbon Nanotubes for Life Sciences Applications. ***ChemSusChem***, 4(7): 848-863.

3- Kum, M.C.; Joshi, K.A.; Chen, W.; Myung, N.V. and Mulchandani, A. (2007). Biomolecules-carbon nanotubes doped conducting polymer nanocomposites and their sensor application. ***Talanta***, 74(3): 370-375.

4- Gladchenko, G.; Karachevtsev, M.; Leontiev, V.; Valeev, V.; Glamazda, A. Y.; Plokhotnichenko, A. and Stepanian, S. (2006). Interaction of fragmented double-stranded DNA with carbon nanotubes in aqueous solution. ***Mol. Phys.***104(20): 3193-3201.

5- Katz, E. and Willner, I. (2004). Biomolecule- functionalized carbon

nanotubes: applications in nanobioelectronics. ***ChemPhysChem,*** 5(8): 1084-1104.

6- Meng, S. and Kaxiras, E. (2009). Interaction of DNA with CNTs: Properties and Prospects for Electronic Sequencing. ***Biosensing Using Nanomaterials,*** 3:67-96

7- Tu, X.; Pehrsson, P. E. and Zhao, W. (2007). Redox reaction of DNA-encased HiPCO carbon nanotubes with hydrogen peroxide: A near infrared optical sensitivity and kinetics study. ***The Journal of Physical Chemistry*** *C, 111*: 17227-17231.

8- Xu, Y.; Pehrsson, P. E.; Chen, L.; Zhang, R. and Zhao, W. (2007). Double-stranded DNA single-walled carbon nanotube hybrids for optical hydrogen peroxide and glucose sensing. ***The Journal of Physical Chemistry*** *C, 111*: 8638-8643.

9- Upadhyay, A.; Chen, S. M.; Ting, T. W. and Peng, Y.Y. (2011). A Biosensor for Hydrogen Peroxide Based on Single walled Carbon Nanotube and Metal Oxide Modified Indium Tin Oxide Electrode. ***Int.J.Electrochem.Sci.***, 6: 3466-3482.

10- Halliwell, B.; Clement, M. V. and Long, L.H. (2000). Hydrogen peroxide in the human body. ***FEBS Lett.,*** *486*: 10-13.

11- Ansari, M. and Datta, A.K**.** (2003). An overview of Sterilization Methods for Packaging Materials Used in Asepits Pachging Systems. ***Trans IChemE,***81: 57.

12- He, F.; Feng, F.; Wang, S.; Li, Y. and Zhu, D. (2007). Fluorescence ratiometric assays of hydrogen peroxide and glucose in serum using conjugated polyelectrolytes. ***Journal of Materials Chemistry*** *, 17*: 3702-3707.

13- Kim, J. H.; Patra, C. R.; Arkalgud, J. R.; Boghossian, A. A.; Zhang, J.; Han, J. H.; Reuel, N. F.; Ahn, J. H.; Mukhopadhyay, D. and Strano, M.S. (2011). Single-Molecule Detection of H2O2 Mediating Angiogenic Redox Signaling on Fluorescent Single-Walled Carbon Nanotube Array. ***ACS nano,*** *5*: 7848-7857.

14- Tabner, B. J.; Turnbull, S.; El-Agnaf, O. and Allsop, D. (2002). Formation of hydrogen peroxide and hydroxyl radicals from A (beta) and alpha-synuclein as a possible mechanism of cell death in Alzheimer's disease and Parkinson's disease. ***Free Radic. Biol. Med.,*** *32*: 1076.

15- Griendling, K. K.; Sorescu, D. and Ushio-Fukai, M. (2000). NAD (P) H oxidase: role in cardiovascular biology and disease**.** ***Circ. Res.,*** *86*: 494-501.

16- Pryor, W.A. (1997). Cigarette smoke radicals and the role of free radicals in chemical carcinogenicity. ***Environ. Health Perspect.,*** *105*: 875.

17- Ahammad, J.S. (2013). Hydrogen Peroxide Biosensors Based on Horseradish Peroxidase and Hemoglobin. ***J Biosens Bioelectron*** *,* 9: 1-11.

18- Jaanus, K.; Vaeino, S. and Banks, C.E. (2008). A systematic study of the electrochemical determination of hydrogen peroxide at single-walled carbon nanotube ensemble networks. ***Electrochemistry Communications***, 10 (12): 1872-1875.

19- Upadhyay, A.K.; Chen, S.M.; Peng, Y.Y. (2011). A Biosensor for Hydrogen Peroxide Based on Single walled Carbon Nanotube and Metal Oxide Modified Indium Tin Oxide Electrode. ***Int. J. Electrochem. Sci***., 6: 3466 – 3482

20- Gao, X.; Jin, L.; Wu,Q.; Chen,Z. and Lin,X. (2012). A Nonenzymatic Hydrogen Peroxide Sensor Based on Silver Nanowires and Chitosan Film. ***Electroanalysis,*** 24(8): 1771 – 1777.

21- Luo, F.; Yin, J.; Gao , F. and Wang, L. (2009). A non-enzyme hydrogen peroxide sensor based on core/shell silica nanoparticles using synchronous fluorescence spectroscopy. ***Microch Acta,***165: 23–28.

22- He, F.; Feng, F.; Wang, S.; Li, Y. and Zhu, D. (2007). Fluorescence ratiometric assays of hydrogen peroxide and glucose in serum using conjugated polyelectrolytes. ***J. Mater. Chem.,***17: 3702–3707.

23- Chai, X. S.; . Hou, Q.X.; Luo, Q. and Zhu, J.Y. (2004). Rapid determination of hydrogen peroxide in the wood pulp bleaching streams by a dual-wavelength spectroscopic method. ***Analytica Chimica Acta***, 507: 281–284.

24- Lee, D.; Erigala, V.R.; Dasari, M.; Yu, J.; Dickson, R.M. and Murthy, N. (2008). Detection of hydrogen peroxide with chemiluminescent micelles. ***International Journal of Nanomedicine,*** 3(4): 471–476.

25- Liu, H.J.; Yanga, D.W. and Liu, H.H. (2012). A hydrogen peroxide sensor based on the nanocomposites of poly(brilliant cresyl blue) and single walled-carbon nanotubes. ***Anal.Methods***, 4: 1421–1426.

26- Kelley, K.; Pehrsson, P.E.; Ericson, L.M. and Zhao, W. (2005). Optical pH Response of DNA Wrapped HiPco Carbon

Nanotubes. ***J. Nanosci. Nanotech,*** 5: 1029-1032.

27- O'Connell, M. J.; Eibergen, E. E. and Doorn, S. K. (2005) .Chiral selectivity in the charge-transfer bleaching of single-walled carbon-nanotube spectra. ***Nat. Mater***., 4: 412-418.

28- Song, C.; Pehrsson, P. E. and Zhao, W. (2005). Recoverable Solution Reaction of HiPco Carbon Nanotubes with Hydrogen Peroxide. ***J. Phys. Chem. B.***, 109: 21634-21639.

29- Pan, S.; Chung, H.; Arnold, M.A. and Small, G. W. (1996). Near-infrared spectroscopic measurement of physiological glucose levels in variable matrices of protein and triglycerides. ***Anal.Chem.****, 68: 1124-1135.*

30- Di Simplicio, P.; Cheeseman, K. and Slater, T. (1991). The reactivity of the SH group of bovine serum albumin with free radicals. ***Free Radic. Res.****, 14*: 253-262.

31- Edri, E. and Regev, O. (2008). pH effects on BSA-dispersed carbon nanotubes studied by spectroscopy-enhanced composition evaluation techniques. ***Anal. Chem.****, 80*: 4049-4054.

32- Carballal, S.; Radi, R.; Kirk, M. C.; Barnes, S.; Freeman, B. A. and Alvarez, B. (2003). Sulfenic acid formation in human serum albumin by hydrogen peroxide and peroxynitrite. ***Biochemistry (N. Y.),*** *42*, 9906-9914.

33- Chandler, J.D and Day, B.J. (2012). THIOCYANATE: A potentially useful therapeutic agent with host defense and antioxidant properties., 84(11): 1381–1387.

34- Aoki, K. and Hori, J. (1962). Precipitation of bovine serum albumin by thiocyanate ion. *Arch.* ***Biochem. Biophys.****, 97*: 75-79.

35- Christy, A.A. and Egeberg, P.K. (2000). Oxidation of thiocyanate by hydrogen peroxide—a reaction kinetic study by capillary electrophoresis. ***Talanta****, 51*: 1049-1058.

36- Thomas, E.L.; Aune, T.M. (1978). Lactoperoxidase, peroxide, thiocyanate antimicrobial system: correlation of sulfhydryl oxidation with antimicrobial action. ***Infect. Immun.,*** *20*: 456-463.

37- Xu, Y.; Pehrsson, P. E.; Chen, L. and Zhao, W. (2008). Controllable Redox Reaction of Chemically Purified DNA− Single Walled Carbon Nanotube Hybrids with Hydrogen Peroxide. ***J. Am. Chem. Soc.****, 130*: 10054-10055.

38- Pacher, P.; Beckman, J.S. and Liaudet, L. (2007). Nitric Oxide and Peroxynitrite in Health and Disease.***Physiol Rev***., 87(1), 315–424.

39- Ho, *et al*. (2008). Protective capacities of certain spices against peroxynitrite-mediated biomolecular damage. ***Food Chem Toxicol,*** 46(3): 920-928.

40- Casey, M.; Davoren, E.; Herzog, F.M.; Lyng, H.J. and Byrne, G. (2007). Chambers, Probing the interaction of single walled carbon nanotubes within cell culture medium as a precursor to toxicity testing, ***Carbon***, 45: 34–40.

41- Strano, M.S. *et al*. (2008). Multimodal optical sensing and analyte specificity using single-walled carbon nanotubes. ***Nature Nanotechnology,*** www.nature.com/nature nanotechnology.